



# Assessing vehicle fuel efficiency using a dense network of CO<sub>2</sub> observations

Helen L. Fitzmaurice<sup>1</sup>, Alexander J. Turner<sup>2</sup>, Jinsol Kim<sup>1</sup>, Katherine Chan<sup>3</sup>, Erin Delaria<sup>4</sup>, Catherine Newman<sup>4</sup>, Paul  
5 Wooldridge<sup>4</sup>, Ronald C. Cohen<sup>1,4</sup>

1. University of California, Berkeley, Department of Earth and Planetary Science

2. University of Washington, Department of Atmospheric Sciences

3. Sacramento Metro Air Quality Management District

4. University of California, Berkeley, Department of Chemistry

10 *Correspondence to:* Ronald C. Cohen (rccohen@berkeley.edu)

**Abstract.** Transportation represents the largest sector of anthropogenic CO<sub>2</sub> emissions in urban areas. Timely reductions in urban transportation emissions are critical to reaching climate goals set by international treaties, national policies, and local governments. Transportation emissions also remain one of the largest contributors to both poor air quality (AQ) and to inequities in AQ exposure. As municipal and regional governments create policy targeted at reducing transportation  
15 emissions, the ability to evaluate the efficacy of such emission reduction strategies at the spatial and temporal scales of neighborhoods is increasingly important. However, the current state of the art in emissions monitoring does not provide the temporal, sectoral, or spatial resolution necessary to track changes in emissions and provide feedback on the efficacy of such policies at a neighborhood scale. The BERkeley Air Quality and CO<sub>2</sub> Network (BEACO<sub>2</sub>N) has previously been shown to provide constraints on emissions from the vehicle sector in aggregate over a ~1300 km<sup>2</sup> multi-city spatial domain. Here, we  
20 focus on a 5 km, high volume, stretch of highway in the SF Bay area. We show that inversion of the BEACO<sub>2</sub>N measurements can be used to understand two factors that affect fuel efficiency: vehicle speed and fleet composition. The CO<sub>2</sub> emission rate of the average vehicle (g/vkm) are shown to vary by as much as 27% at different times of a typical weekday because of changes in vehicle speed and fleet composition. The BEACO<sub>2</sub>N-derived emissions estimates are consistent to within ~3% of estimates derived from publicly available measures of vehicle type, number, and speed,  
25 providing direct observational support for the accuracy of the Emissions FACTor model (EMFAC) of vehicle fuel efficiency.

## 1 Introduction

Urban emissions currently account for ~75 % of all anthropogenic CO<sub>2</sub> emissions (IPCC, 2014). By 2050, roughly two-thirds of the earth's projected population of 9.3 billion is expected to reside within urban areas (IPCC, 2014), meaning that effective greenhouse gas emissions reductions strategies must focus on urban emissions reductions.



30 The transportation sector is responsible for ~23% of global greenhouse gas emissions worldwide (IPCC, 2014) and  
represents the greatest sectoral percentage (~25-66%) of emissions from within the boundaries of urban areas in the United  
States (Daw, 2020; Kevin Robert Gurney et al., 2021). Although fuel efficiency of new internal combustion engine vehicles  
has increased by ~30% over the last 20 years and electric vehicles (EV) are becoming more prevalent  
(<https://arb.ca.gov/emfac/emissions-inventory>), emissions reductions resulting from fuel efficiency gains in newer vehicles  
35 are negated by an increasing percentage of heavy-duty vehicles (HDV) (Moua, 2018), speed-related reductions in fuel  
efficiency resulting from increases in congestion, and an increase of total vehicle kilometers travelled (vkm). Over the past  
20 years, even in locations with aggressive climate change policy, these factors have resulted in per capita CO<sub>2</sub> emissions  
from vehicles that have increased or stayed constant. For example, California Air Resources Board estimates that in the state  
of California, per capita vehicle emissions in 2015 were only 2% lower than in 2000 and per capita vehicle kilometers  
40 traveled (vkm) increased ~2.5% over that time period (California Air Resources Board, 2018). In addition to GHG  
emissions, the transportation sector is responsible for a significant share of PM<sub>2.5</sub> and NO<sub>x</sub> emissions, exacerbating PM<sub>2.5</sub> and  
ozone exposure in low-income communities and communities of color already experiencing disproportionate health burdens  
associated with poor air quality (Tessum et al., 2021).

Municipal and regional governments have increasingly shown interest in tracking and reducing CO<sub>2</sub> emissions from  
45 all sectors, including transportation. For example, Boswell (Boswell & Madilyn Jacobson, 2019) found that 64% of  
Californians live in a city with a climate action plan. For urban and regional governments to plan, monitor, and responsively  
adjust emissions reduction policies, an up-to-date understanding of the spatial and temporal variations in total emissions and  
in emissions by sector and subsector processes is key.

For transportation, reductions in vkm, congestion mitigation, and rules affecting fleet composition (e.g., limiting  
50 road access to HDV, incentivizing use of electric vehicles, or buy-backs of older vehicles) are three levers that can be  
employed to reduce CO<sub>2</sub> and AQ emissions from vehicles, thereby affecting the climate footprint, air quality (AQ), and  
environmental justice (EJ) in a region. However, the current state of the art in emissions monitoring and modelling do not  
provide the temporal, sectoral, or spatial resolution necessary to track changes in urban emissions and provide feedback on  
the efficacy of each lever separately. Furthermore, current estimates of the magnitude and sectoral apportionment, of urban  
55 CO<sub>2</sub> emissions can vary widely (3, 8). For example, Gurney et al. show how a consistent approach to total emissions from  
cities across the U.S. differs from locally constructed inventories in magnitude and sector by sector (Kevin Robert Gurney et  
al., 2021).

Spatial and temporal process-level maps of emissions are needed to improve the scientific basis for emission control  
strategies. The current state of the art involves finding aggregate traffic emissions over large regions (counties, states) using  
60 economic data and downscaling those totals using either vehicle flow rates or proxies like road length and population  
density. These models meet the need for high spatial resolution (~500 m) and capture emissions from many detailed  
subsectors (Conor K. Gately, Hutyra, & Wing, 2015; Kevin R. Gurney et al., 2012; McDonald, McBride, Martin, & Harley,



2014). Because fuel sales are well-characterized, these models are also likely to produce accurate region-wide CO<sub>2</sub> emissions totals.

65 Yet even the most detailed of these inventories do not presently describe the temporal variability in processes that affect emissions, such as the direct response of home heating or air conditioning to ambient temperature or, with one exception (Conor K. Gately, Hutyra, Peterson, & Sue Wing, 2017), the variations in emissions per km when comparing free-flowing to stop-and-go traffic. These models often disagree with one another spatially (C. K. Gately & Hutyra, 2017), and for the most part, are not tested against observations of the atmosphere, and are not designed to be consistent with separately  
70 constructed AQ inventories that have been subject to extensive testing against observations.

Mobile monitoring campaigns and high-density measurement networks highlight the importance of characterizing and identifying the processes contributing to sharp neighborhood-scale AQ and GHG hotspots and point to the importance of traffic emissions on this scale. For example, Apte et al, showed that concentrations of NO<sub>x</sub> and BC can vary by as much as a factor of ~8 on the scale of 10s to 100s of meters (Apte et al., 2017), Caubel et al, showed BC concentrations to be ~2.5  
75 times higher on trucking routes than on neighboring streets (Caubel, Cados, Preble, & Kirchstetter, 2019). Such gradients are not represented in inventories based on downscaled economic data.

Observations of CO<sub>2</sub> and other greenhouse gases can play an important role in improving and maintaining the accuracy of emission models—especially during a time of rapid proposed changes. CO<sub>2</sub> measurements paired with Bayesian inverse models have been shown to provide a quantitative assessment of emissions (Lauvaux et al., 2020, 2016; Turner, Kim, et al., 2020). To date, most attempts at quantifying urban CO<sub>2</sub> emissions have focused on extracting a temporally averaged (often a full year) total of the anthropogenic CO<sub>2</sub> across the full extent of city. A few studies have attempted to disaggregate emissions by sector or describe large shifts in aggregate emissions (Lauvaux et al., 2020; Turner, Kim, et al., 2020), but none characterize subsector processes.

High spatial density observations offer promise as a means to explore process-level emissions details. The BERkeley Air Quality and CO<sub>2</sub> Network (BEACO<sub>2</sub>N) is an observing network deployed in the San Francisco Bay Area and other cities with measurement spacing of ~2km (Figure 1, left). In a prior analysis, Turner et al. (Turner, Kim, et al., 2020) showed that BEACO<sub>2</sub>N measurements can detect variation in CO<sub>2</sub> emissions with time of day and day of week in addition to the dramatic changes in CO<sub>2</sub> emissions due to the COVID-related decrease in driving.

Here, we analyze hourly, spatially-allocated CO<sub>2</sub> emissions derived from the inversion of BEACO<sub>2</sub>N observations  
90 (Turner, Kim, et al., 2020) to explore how well they constrain the CO<sub>2</sub> emissions from a 5km stretch of highway where emissions are affected by speed (vehicles use more fuel per km at very low and high speeds) and fleet-composition (HDV emit more CO<sub>2</sub> per km than light duty vehicles (LDV)). The variation of the ratio of total fleet CO<sub>2</sub> emission per vehicle km traveled (CO<sub>2</sub>/vkm) is used to explore variations in on-road fuel efficiency and the factors responsible for that variation. We show that average fuel efficiency of the vehicle fleet on the road varies by as much as 27% over the course of a typical  
95 weekday.



## 2 Methods and Data

### 2.1 The Berkeley Air quality and CO<sub>2</sub> Network

We use hourly CO<sub>2</sub> observations from the Berkeley Air quality and CO<sub>2</sub> Network (BEACO<sub>2</sub>N) (Delaria et al., 2021; Kim, Shusterman, Lieschke, Newman, & Cohen, 2018; Shusterman et al., 2016). The BEACO<sub>2</sub>N network includes more than 70 locations in the SF Bay Area, spaced at ~2 km, and CO<sub>2</sub> measurements at individual sites have been shown to be accurate to 1.6 ppm (Delaria et al., 2021). All available data from January-June 2018-2020 are included in this analysis. During this time, more than 50 nodes were active for a month or more (including 19 sites within 10 km of our highway stretch of interest). The number of nodes active at any given time ranged from 7-41, with a mean of 17. Figure 1 shows sites in operation at some point during analysis period and timeseries of number of sites actively reporting data.

### 2.2 The BEACO<sub>2</sub>N - STILT Inversion System

To infer CO<sub>2</sub> emissions from within the BEACO<sub>2</sub>N footprint, we use the Stochastic-Time Inverted Lagrangian Transport (STILT) model, coupled with a Bayesian inversion as described in detail in Turner et al 2020a (Turner, Kim, et al., 2020). Briefly, we use meteorology from NOAA's HRRR product at 3 km resolution to calculate footprints from each hour at each site, weighted by a priori CO<sub>2</sub> emissions. The overall region of influence, the network footprint, as defined by a contour representing 40% of the CO<sub>2</sub> influence is shown in Figure S1 (left). We construct a spatially gridded prior emissions inventory using point sources provided by the Bay Area Air Quality Management District (2011), home heating emissions as reported by BAAQMD (2011) and distributed spatially according to population density, on-road emissions from the High-resolution Fuel Inventory for Vehicle Emissions (McDonald et al., 2014) varying by hour of week and scaled by year using fuel sales data, and a biogenic inventory derived using Solar Induced Fluorescence (SIF) Satellite data (Turner, Köhler, et al., 2020).

To ensure a focus on highway emissions, we subtract prior estimates associated with non-highway sources from posterior BEACO<sub>2</sub>N-STILT fluxes. Non-highway sources are small (~12%) in comparison with highway emissions. We assume that the error in prior estimates to be even smaller.

We estimate BEACO<sub>2</sub>N-STILT inversion to be precise to at least 30% for a line source. This estimate is based on the results of Turner (2016) (Turner et al., 2016) who used Observation System Simulation Experiments to demonstrate that with 7 days of observations at 30 sites a 45 tC/hr line source could be constrained to 15 t C/hr. However, this paper also demonstrated that error in the posterior decreased as results were averaged over a longer period of time, and because we are using 18 months, rather than 7 days of observations, we expect and observe better precision than this.

### 2.3 PeMS-EMFAC – derived CO<sub>2</sub> Emissions Estimates

Total hourly vehicle flow, truck (HDV) percent, and speed, were retrieved from <http://pems.dot.ca.gov> for January – June 2018-2020. There are ~1800 traffic counting stations hosted by the Caltrans Performance Measurement System (PeMS) in the Bay Area, including more than 400 sites (Fig S1) within the 2020 footprint of the BEACO<sub>2</sub>N, as described in Turner



(2020a) (Turner, Kim, et al., 2020). These stations count vehicle flow using magnetic loops imbedded in roadways and estimate HDV fraction using calculated vehicle speed and assumptions about vehicle length (Kwon, Varaiya, & Skabardonis, 2003). For hours during which fewer than 50% of measurements were reported, we fill in total speed and light duty vehicle (LDV) flow gaps by using linear fits to nearest neighbor sites and gaps in HDV flow using hour-of-day- and weekend/weekday-specific median ratios between neighboring sites. We calculate both LDV and HDV vkm for each highway segment during each hour, using downloaded flow data at each sensor location and segment lengths obtained from the PeMS database. For highway segments within the BEACO<sub>2</sub>N footprint, vkm are summed to obtain regional highway HDV and LDV vkm for every hour. Figure 2 (left) shows the extent of the PeMS network in comparison to the BEACO<sub>2</sub>N-STILT footprint. In Figure 2 (right), we show total HDV vkm and LDV vkm.

Vehicle fuel efficiency is dependent on both fleet composition and vehicle speed. We calculate an emissions rate at each location by combining speed and the HDV percentage with fuel efficiency estimates provided by the California Air Resources Board's Emissions FACTor Model (EMFAC2017). The EMFAC2017 model provides yearly fuel efficiency estimates for the Bay Area for 41 vehicle classes as a function of speed. We group these 41 vehicle types into the categories LDV or HDV. (Table S1) PeMS's vehicle-type classification system is length based, assuming that LDV have a median length of 3.7 m and HDV a median length of 18.3 m (Kwon et al., 2003). As a result, we group most light duty trucks into the LDV category. To find speed-dependent emissions rate values for the LDV and HDV groups, we find a vkm-weighted mean of emissions rates across all vehicle-classes within a group at a given speed

$$er(speed, group) = \frac{\sum_{i=1}^n vkm_i er_i}{\sum_{i=1}^n vkm_i}, \quad (1)$$

where  $i$  is a vehicle class. From this, we generate LDV and HDV emissions rates at 8.02 kph (5 mph) intervals.

Because EMFAC does not provide data for several LDV vehicle classes at and above 96.8 kph (60 mph) we estimate emissions rates for the LDV group by using emissions rate to speed slopes ( $\text{g CO}_2 \text{ vkm}^{-1} \text{ kph}^{-1}$ ) for high speeds (88-145 kph), using data from Argonne National Lab and EPA (Davis, Diegel, & Boundy, 2021).

We then calculate emissions rates ( $\text{g CO}_2 / \text{vkm}$ ) for each road segment at a moment in time

$$er(t, seg) = \frac{vkm_{LDV}(t, seg) er_{LDV}(t, seg) + vkm_{HDV}(t, seg) er_{HDV}(t, seg)}{vkm_{LDV}(t, seg) + vkm_{HDV}(t, seg)}, \quad (2)$$

where emissions rates for cars and trucks are found via spline fit between reported speed for that segment and time with our curves for the emissions rates of each vehicle class.

From the emissions rate for each segment, we calculate emissions rate for a stretch of highway including several segments to find total emissions rate ( $er$ ) along a "stretch" over a period of time:

$$er(t, stretch) = \frac{\sum_{all\ segments} vkm_{LDV}(t, s) er_{LDV}(t, s) + vkm_{HDV}(t, s) er_{HDV}(t, s)}{\sum_{all\ segments} vkm_{LDV}(t, s) + vkm_{HDV}(t, s)}. \quad (3)$$

Total CO<sub>2</sub> emissions for the highway stretch analyzed in this work are shown in Figure 2b.



### 3 Results

To gain insight into the relative impacts of congestion and fleet composition, we calculate fleet-wide vehicle emission rates ( $\text{gCO}_2/\text{vkm}$ ) using two different methods. For both methods, the Caltrans Performance Measurement System (PeMS) provides vehicle counts, speed and categorizes HDV vs. LDV (<http://pems.dot.ca.gov>). Using this data and estimates of fuel  
165 per km from the EMISSIONS FACTOR 2017 (EMFAC) Model, we calculate the  $\text{CO}_2$  emissions per km for the average vehicle with hourly time resolution as described above. Second, we use the PeMS data in combination with  $\text{g CO}_2$  per unit area derived from the BEACO<sub>2</sub>N-STILT inversion system. We focus on the ~5 km stretch of Interstate-80 just north of the San Francisco-Oakland Bay Bridge (Figure 2). The road has 5 lanes in each direction and is often subject to high congestion and slow speeds.

170 PeMS-EMFAC-derived emissions rates give us insight into (1) the expected variation in emissions rates across a typical day and (2) the relative impacts of congestion vs. HDV percentage as factors leading to this variation (Figure 2). For example, while the west-bound segment experiences speeds significantly below free-flow during both morning and evening rush hours, the east-bound segment experiences significant congestion only during the evening. The west-bound congestion in this segment occurs at speeds that are more efficient than free-flow. The overall variance in emissions rates over the whole  
175 stretch is significantly smaller than in either of the directions shown individually.

From PeMS-EMFAC-derived emissions factors, we predict a median diel cycle with emissions per km travelled ranging from ~247 to ~314  $\text{g CO}_2 / \text{vkm}$ . For reference, if all vehicles were driving at the speed limit of 104.6 kph (65 mph) and the fleet mix was 6% HDV and 94% LDV, we calculate an emission rate of 265  $\text{g CO}_2 / \text{vkm}$ . The range of predicted emissions are narrower on the weekend (238 to 276  $\text{g CO}_2 / \text{vkm}$ ), both because fewer HDV use the road and because there  
180 is a smaller range in speed.

We use  $\text{CO}_2$  measurements from 50 BEACO<sub>2</sub>N sites across the Bay Area, combined with the BEACO<sub>2</sub>N-STILT inversion system to estimate highway emissions from our stretch of interest. In Figure 1, we show the location of BEACO<sub>2</sub>N sites, the stretch of interest, and emissions estimates for this stretch. Note that the posterior emissions estimates move substantially from prior emissions towards what is estimated from PeMS-EMFAC, particularly during evening rush hour,  
185 during which the prior overestimates emissions by ~20%.

We compare BEACO<sub>2</sub>N-derived and PeMS-EMFAC-derived emissions rates ( $\text{CO}_2 / \text{vkm}$ ) and find remarkable agreement. The PeMS-EMFAC-derived emissions rates range from 225-300  $\text{g CO}_2 / \text{vkm}$  and include effects of both fleet composition and variation in speed. For BEACO<sub>2</sub>N, we use the total  $\text{CO}_2$  emissions from the inversion at times corresponding to narrow bins of PeMS-EMFAC  $\text{g CO}_2 / \text{vkm}$ . Figure 3 (left) shows an example of data selected with PeMS-  
190 EMFAC-derived fuel efficiency in the range 271.4-279  $\text{g CO}_2 / \text{vkm}$ . There is a range of emissions at each vkm because of noise in the inversion, variation in speed and variation in fleet composition. The slope of a fit to the data in Figure 3 (left) is an estimate of the emissions rate (equation 4), where  $\text{CO}_2$  emissions is defined as hourly emissions summed over BEACO<sub>2</sub>N pixels corresponding to our highway stretch of interest (Figure 3).



$$CO_2/vkm = \frac{CO_2 \text{ emissions}}{vkm}, \quad (4)$$

195 Using 18 months of data for all hours between 4 am and 10 pm, we compare PeMS-EMFAC-derived and BEACO<sub>2</sub>N-derived CO<sub>2</sub> / vkm (Figure 3, right). Fitting to a line forced through the origin, emissions rates found via the BEACO<sub>2</sub>N inversion are within 3% (0.97 +/- 0.01) of those predicted using PeMS-EMFAC traffic counts. Because eight of the nine points corresponding to emission rate bins fall within 5% of the fit, we estimate that the BEACO<sub>2</sub>N system would be able to detect a change in emission rates on the order of 5%.

200 We also consider how emissions rates agree throughout the day (Figure 4, top). During the evening, PeMS-EMFAC-derived and BEACO<sub>2</sub>N-derived emission rates are in good agreement. The BEACO<sub>2</sub>N CO<sub>2</sub>/vkm increases from 256 g CO<sub>2</sub> / vkm before rush hour (2 pm) to 324 g CO<sub>2</sub>/vkm during peak rush hour (5 pm). Likewise, the PeMS-EMFAC-derived CO<sub>2</sub>/vkm increases from 256 CO<sub>2</sub> / vkm to 320 CO<sub>2</sub> / vkm over the same time period. The BEACO<sub>2</sub>N prior has a slightly higher emission rates over this period (256 g CO<sub>2</sub>/vkm to 361 g CO<sub>2</sub>/vkm).

205 In contrast, during the morning rush hours, we see less agreement between PeMS-EMFAC-derived and BEACO<sub>2</sub>N-derived emission rate estimates. The BEACO<sub>2</sub>N inversion is similar to the PeMS-EMFAC estimate at 5 am local time (280 g CO<sub>2</sub> / vkm) and then increases over the morning rush hour to 330 g CO<sub>2</sub> / vkm at 8 am. This behavior is different than either the BEACO<sub>2</sub>N prior (175 at 5 am and 275 at 8 am) or the PeMS-EMFAC calculation which decreases over this period (275 at 5 am and 250 at 8 am).

210 The discrepancy in the morning between emissions derived from PeMS-EMFAC and BEACO<sub>2</sub>N can potentially be reconciled by congestion. There is a non-linear relationship between vehicle speed and the rate of emissions. As such, congestion involving non-constant speeds can result in higher emissions than would be estimated using the average vehicle speed. This can be seen from a simple example. Consider two cases: 1) a LDV travelling at a constant 50 kph for one hour and 2) a LDV traveling at 100 kph for 20 minutes and 25 kph for 40 minutes. Both vehicles travel 50 km in 1 hour and  
215 therefore have the same average speed. However, the emissions rate is 461.5 g CO<sub>2</sub>/vkm at 25 kph, 195 g CO<sub>2</sub>/vkm at 50 kph, and 221 g CO<sub>2</sub>/vkm at 100 kph. Using these emission rates, the vehicle in the first case would emit 9.75 kg CO<sub>2</sub> whereas the vehicle with the variable speed in the second case would emit 15 kg CO<sub>2</sub>.

#### 4 Discussion

Strategic reduction of emissions from transportation is important to both reducing total GHG emissions and improving AQ.  
220 To make informed decisions that reduce GHGs and exposure to poor AQ, policy makers need to know (1) how much is being emitted, (2) location and timing of emissions, and (3) the relative impact of various sub-sector processes (vkm, fleet composition, congestion).

To effectively capture emissions from sub-sector processes, models are also reliant on emissions factor models, such as the EMFAC2017 emissions model used in this paper. While our measurements largely agreed with the EMFAC2017  
225 emissions model for CO<sub>2</sub>, plume-based emission factor measurements of co-emitted pollutants (CO, NO<sub>x</sub>, PM<sub>2.5</sub>, BC,



NMHC) show various emissions factor models to systematically underestimate emissions factors (Bishop, 2021), fail to capture spatial heterogeneity in these factors due to fleet composition (age and compliance with control technologies) for PM (Haugen & Bishop, 2018; Park, Vijayan, Mara, & Herner, 2016) and Black Carbon (Preble, Cados, Harley, & Kirchstetter, 2018), or fail to capture the impact of temperature on emissions factors.

230 Tracking on-road changes in emission factors will be especially important as the impacts of congestion and fleet composition evolve rapidly in interactive ways, making timely updates essential to creating spatially accurate inventories. For example, the EMFAC model predicts an 18% decrease in overall CO<sub>2</sub> emission rates by 2030, resulting from the improved fuel efficiency of combustion engine vehicles and a transition to hybrid and EV (~6.8% of LDV vkm and ~6% of HDV vkm are expected to be travelled by EV by 2030). While the increased share of hybrid and EV should work to decrease  
235 the impact of congestion, a projected increase in total congestion and congested-vkm share by HDV (Texas A&M Transportation Institute, 2019) is likely to work against that trend, making the overall result difficult to predict.

To our knowledge, this paper represents the first demonstration that a high-density surface network can both diagnose and quantify relative contributions of sub-sector processes at the neighborhood scale using atmospheric data. We demonstrate that atmospheric measurements, specifically a dense network (~2 km spacing) of low-cost CO<sub>2</sub> sensors, can be  
240 used to quantify emission rates at a specific location (~5 km stretch) and by time of day. We show that on the highway stretch, activity-based emissions estimates that account for speed and HDV % match the inference from atmospheric measurements to within 3%. Finally, we demonstrate that the BEACO<sub>2</sub>N-STILT system detects changes in fuel efficiency that range from 200-300 g CO<sub>2</sub> / vkm and that these variations are accurate to within approximately 5%.

Applying these methods across a broader spatial area and to other species (PM<sub>2.5</sub>, NO<sub>x</sub>, CO) should yield information of  
245 interest to both scientists and policy makers by:

1. Revealing spatial and temporal trends in CO<sub>2</sub> emissions rates across an urban area and quantifying spatially the contributions of congestion, fleet composition, or other factors.
2. Identifying and diagnosing the causes of traffic-related AQ hotspots that contribute to exposure inequities.
3. Characterizing emissions rates and emissions factors as a function of location, congestion, fleet composition, or  
250 meteorology.
4. Tracking trends in the above over periods of years to decades.

#### Author Contributions:

HLF derived CO<sub>2</sub> emissions from traffic data, conceived of project design, wrote manuscript, collected CO<sub>2</sub> data. AJT  
255 created and ran CO<sub>2</sub> inversion code. HLF, JK, KC, ED, CN, PW collected CO<sub>2</sub> data. RCC gave feedback on project design, assisted in writing manuscript.

**Competing Interest Statement:** We have no competing interests to disclose.



260 **Acknowledgments:** HLF was supported by NSF GRFP fellowship and Microsoft Research Internship. Thanks to K. Lauter and MSR Urban Innovation Group for support in thinking through PeMS data acquisition. AJT was supported as a Miller Fellow with the Miller Institute for Basic Research in Science at UC Berkeley. This research was funded by grants from the Koret Foundation and University of California, Berkeley. This research used the Savio computational cluster resource provided by the Berkeley Research Computing program at the University of California, Berkeley (supported by the UC  
265 Berkeley Chancellor, Vice Chancellor for Research, and Chief Information Officer). Thanks to HSK for reading through and offering organizational suggestions on the manuscript.

**Data Availability:** The CO<sub>2</sub> data used for this study are publicly available at <http://beacon.berkeley.edu> (Cohen Research, 2021). Raw data can be given upon request. The traffic data used for this study is publicly available at <https://pems.dot.ca.gov/>.

## 270 References

- Apte, J. S., Messier, K. P., Gani, S., Brauer, M., Kirchstetter, T. W., Lunden, M. M., ... Hamburg, S. P. (2017). High-Resolution Air Pollution Mapping with Google Street View Cars: Exploiting Big Data. *Environmental Science and Technology*, 51(12), 6999–7008. <https://doi.org/10.1021/acs.est.7b00891>
- Bishop, G. A. (2021). Does California's EMFAC2017 vehicle emissions model underpredict California light-duty gasoline  
275 vehicle NO<sub>x</sub> emissions? *Journal of the Air and Waste Management Association*, 71(5), 597–606. <https://doi.org/10.1080/10962247.2020.1869121>
- Boswell, M. R., & Madilyn Jacobson, A. R. (2019). 2019 Report on the State of Climate Action Plans in California FINAL REPORT Principal Investigator, (17).
- California Air Resources Board. (2018). 2018 PROGRESS REPORT: California's Sustainable Communities and Climate  
280 Protection Act, (November), 96. Retrieved from <https://ww2.arb.ca.gov/legislatively-mandated-reports>
- Caubel, J. J., Cados, T. E., Preble, C. V., & Kirchstetter, T. W. (2019). A Distributed Network of 100 Black Carbon Sensors for 100 Days of Air Quality Monitoring in West Oakland, California. *Environmental Science and Technology*, 53(13), 7564–7573. <https://doi.org/10.1021/acs.est.9b00282>
- Davis, S. C., Diegel, S. W., & Boundy, R. G. (2021). *Transportation Energy Data Book, Edition 29*. Energy.
- 285 Daw, T. (2020). Oakland EQUITABLE CLIMATE ACTION PLAN, (July).
- Delaria, E. R., Kim, J., Fitzmaurice, H. L., Newman, C., Wooldridge, P. J., Worthington, K., & Cohen, R. C. (2021). The Berkeley Environmental Air-quality and CO<sub>2</sub> Network: field calibrations of sensor temperature dependence and assessment of network scale CO<sub>2</sub> accuracy, (May), 1–30.
- Gately, C. K., & Hutyrá, L. R. (2017). Large Uncertainties in Urban-Scale Carbon Emissions. *Journal of Geophysical  
290 Research: Atmospheres*, 122(20), 11,242–11,260. <https://doi.org/10.1002/2017JD027359>



- Gately, Conor K., Hutryra, L. R., Peterson, S., & Sue Wing, I. (2017). Urban emissions hotspots: Quantifying vehicle congestion and air pollution using mobile phone GPS data. *Environmental Pollution*, 229, 496–504. <https://doi.org/10.1016/j.envpol.2017.05.091>
- 295 Gately, Conor K., Hutryra, L. R., & Wing, I. S. (2015). Cities, traffic, and CO<sub>2</sub>: A multidecadal assessment of trends, drivers, and scaling relationships. *Proceedings of the National Academy of Sciences of the United States of America*, 112(16), 4999–5004. <https://doi.org/10.1073/pnas.1421723112>
- Gurney, Kevin R., Razlivanov, I., Song, Y., Zhou, Y., Benes, B., & Abdul-Massih, M. (2012). Quantification of fossil fuel CO<sub>2</sub> emissions on the building/street scale for a large U.S. City. *Environmental Science and Technology*, 46(21), 12194–12202. <https://doi.org/10.1021/es3011282>
- 300 Gurney, Kevin Robert, Liang, J., Roest, G., Song, Y., Mueller, K., & Lauvaux, T. (2021). Under-reporting of greenhouse gas emissions in U.S. cities. *Nature Communications*, 12(1), 1–7. <https://doi.org/10.1038/s41467-020-20871-0>
- Haugen, M. J., & Bishop, G. A. (2018). Long-Term Fuel-Specific NO<sub>x</sub> and Particle Emission Trends for In-Use Heavy-Duty Vehicles in California. *Environmental Science and Technology*, 52(10), 6070–6076. research-article. <https://doi.org/10.1021/acs.est.8b00621>
- 305 IPCC. (2014). *Climate Change 2014 Part A: Global and Sectoral Aspects. Climate Change 2014: Impacts, Adaptation, and Vulnerability. Part A: Global and Sectoral Aspects. Contribution of Working Group II to the Fifth Assessment Report of the Intergovernmental Panel on Climate Change*. Retrieved from [papers2://publication/uuid/B8BF5043-C873-4AFD-97F9-A630782E590D](https://www.ipcc.ch/publications_and_materials/publications_and_materials/publication/uuid/B8BF5043-C873-4AFD-97F9-A630782E590D)
- Kim, J., Shusterman, A. A., Lieschke, K. J., Newman, C., & Cohen, R. C. (2018). The Berkeley Atmospheric CO<sub>2</sub> Observation Network: Field calibration and evaluation of low-cost air quality sensors. *Atmospheric Measurement Techniques*, 11(4), 1937–1946. <https://doi.org/10.5194/amt-11-1937-2018>
- 310 Kwon, J., Varaiya, P., & Skabardonis, A. (2003). Estimation of Truck Traffic Volume from Single Loop Detectors with Lane-to-Lane Speed Correlation. *Transportation Research Record*, 684(1856), 106–117. <https://doi.org/10.3141/1856-11>
- 315 Lauvaux, T., Gurney, K. R., Miles, N. L., Davis, K. J., Richardson, S. J., Deng, A., ... Turnbull, J. (2020). Policy-relevant assessment of urban CO<sub>2</sub> emissions. *Environmental Science and Technology*, 54(16), 10237–10245. <https://doi.org/10.1021/acs.est.0c00343>
- Lauvaux, T., Miles, N. L., Deng, A., Richardson, S. J., Cambaliza, M. O., Davis, K. J., ... Wu, K. (2016). High-resolution atmospheric inversion of urban CO<sub>2</sub> emissions during the dormant season of the Indianapolis flux experiment (INFLUX). *Journal of Geophysical Research*, 121(10), 5213–5236. <https://doi.org/10.1002/2015JD024473>
- 320 McDonald, B. C. (University of C. B., McBride, Z. (University of C. B., Martin, E. (University of C. B., & Harley, R. (University of C. B. (2014). Journal of Geophysical Research: Atmospheres carbon dioxide emissions. *Journal of Geophysical Research: Atmospheres*, (May), 5283–5298. <https://doi.org/10.1002/2013JD021219>.Received
- Moua, F. (2018). *California Annual Fuel Outlet Report Results (CEC-A15)*, Energy Assessments Division, California Energy



- 325      *Comission.*
- Park, S. S., Vijayan, A., Mara, S. L., & Herner, J. D. (2016). Investigating the real-world emission characteristics of light-duty gasoline vehicles and their relationship to local socioeconomic conditions in three communities in Los Angeles, California. *Journal of the Air and Waste Management Association*, 66(10), 1031–1044. <https://doi.org/10.1080/10962247.2016.1197166>
- 330      Preble, C. V., Cados, T. E., Harley, R. A., & Kirchstetter, T. W. (2018). In-Use Performance and Durability of Particle Filters on Heavy-Duty Diesel Trucks. *Environmental Science and Technology*, 52(20), 11913–11921. research-article. <https://doi.org/10.1021/acs.est.8b02977>
- Shusterman, A. A., Teige, V. E., Turner, A. J., Newman, C., Kim, J., & Cohen, R. C. (2016). The Berkeley Atmospheric CO<sub>2</sub> Observation Network: Initial evaluation. *Atmospheric Chemistry and Physics*, 16(21), 13449–13463. <https://doi.org/10.5194/acp-16-13449-2016>
- 335      Tessum, C. W., Paoletta, D. A., Chambliss, S. E., Apte, J. S., Hill, J. D., & Marshall, J. D. (2021). PM<sub>2.5</sub> pollutants disproportionately and systemically affect people of color in the United States. *Science Advances*, 7(18), 1–7. <https://doi.org/10.1126/sciadv.abf4491>
- Texas A&M Transportation Institute. (2019). Urban Mobility Report 2019, 182. Retrieved from [http://web.minienm.nl/mob2015/documents/Mobiliteitsbeeld\\_2015.pdf](http://web.minienm.nl/mob2015/documents/Mobiliteitsbeeld_2015.pdf)
- 340      Turner, A. J., Kim, J., Fitzmaurice, H., Newman, C., Worthington, K., Chan, K., ... Cohen, R. C. (2020). Observed Impacts of COVID-19 on Urban CO<sub>2</sub> Emissions. *Geophysical Research Letters*, 47(22), 1–6. <https://doi.org/10.1029/2020GL090037>
- Turner, A. J., Köhler, P., Magney, T. S., Frankenberg, C., Fung, I., & Cohen, R. C. (2020). A double peak in the seasonality of California’s photosynthesis as observed from space. *Biogeosciences*, 17(2), 405–422. <https://doi.org/10.5194/bg-17-405-2020>
- 345      Turner, A. J., Shusterman, A. A., McDonald, B. C., Teige, V., Harley, R. A., & Cohen, R. C. (2016). Network design for quantifying urban CO<sub>2</sub> emissions: Assessing trade-offs between precision and network density. *Atmospheric Chemistry and Physics*, 16(21), 13465–13475. <https://doi.org/10.5194/acp-16-13465-2016>
- 350



## Figures and Tables

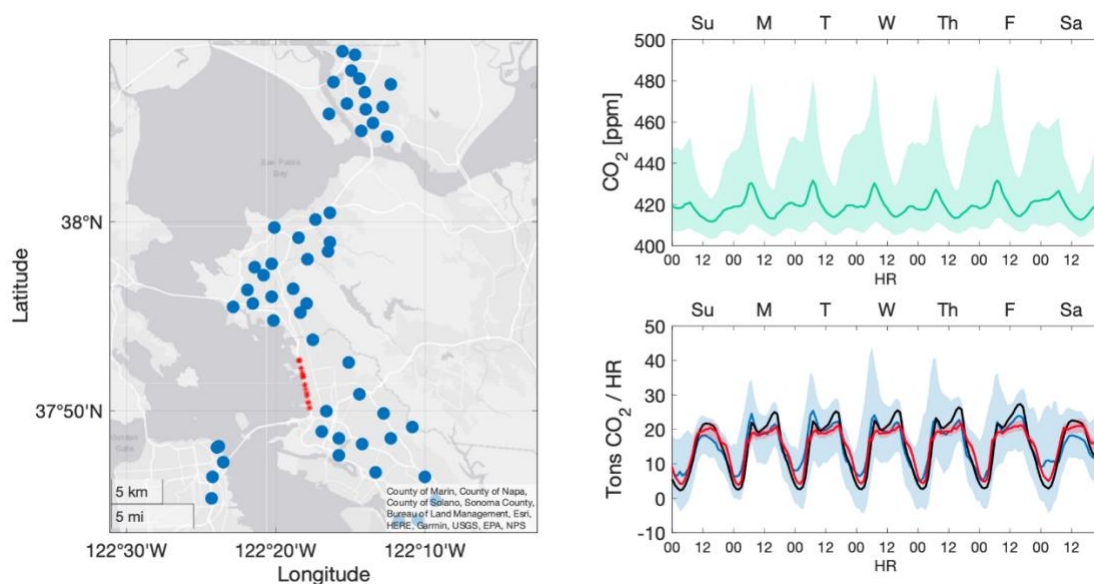
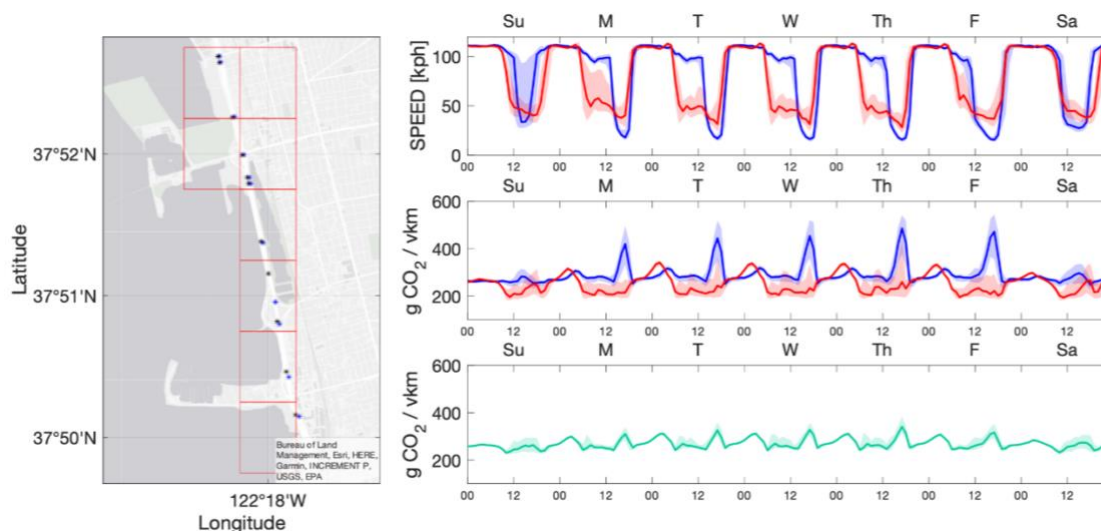


**Figure 1.** Left: Map of the BEACO<sub>2</sub>N Network shows all sites for which there are more than 4 weeks of data during the period analyzed (Jan-June 2018-2020). Right (top): CO<sub>2</sub> values shown for a ‘typical week’ during time period observed. Dark line represents the median value observed across all sites and times. Shaded envelope represents 1 sigma variance across the network and over the 2 year period. Right (bottom): CO<sub>2</sub> emissions on all highway pixels in the domain as derived from the inversion of BEACO<sub>2</sub>N observations (blue), BEACO<sub>2</sub>N prior (black), and PeMS-EMFAC-based estimate (red). Shaded envelope shows variance in emissions during the 18-month analysis window.



360 **Figure 2:** Left: ~5km stretch over which we analyze  $CO_2/km$ . Points show the location of PeMS stations. Squares show  
pixels associated with BEACO<sub>2</sub>N STILT output which we use for comparison. Right (top): Hourly average speed shown for  
two opposite (West in red, East in blue) PeMS measurement stations for a typical week. Right (middle): PeMS-EMFAC-  
derived emissions rates calculated for two opposite (West in red, East in blue) PeMS measurement stations for a typical  
week. Right (bottom) Aggregate PeMS-EMFAC-derived estimated emissions rates from the two directions of traffic for a  
365 typical week for this highway stretch.

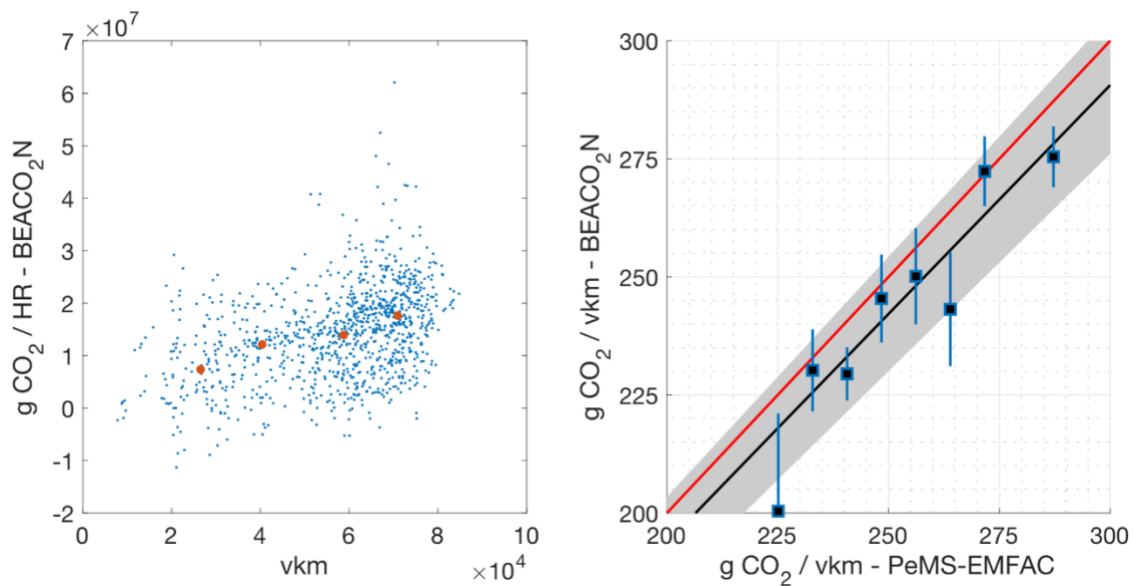


**Figure 3:** Left: BEACO<sub>2</sub>N-derived emissions vs. vkm for times corresponding to modeled emission rates of 271.4-279 g CO<sub>2</sub>/ vkm. Right: BEACO<sub>2</sub>N-derived vs. PeMS-EMFAC derived emissions rates with uncertainty estimate. Black line shows fit weighted by variance:  $y = 0.97(.01)x$ . Grey envelope is 5% deviation from fit. Red line represents 1:1 line.

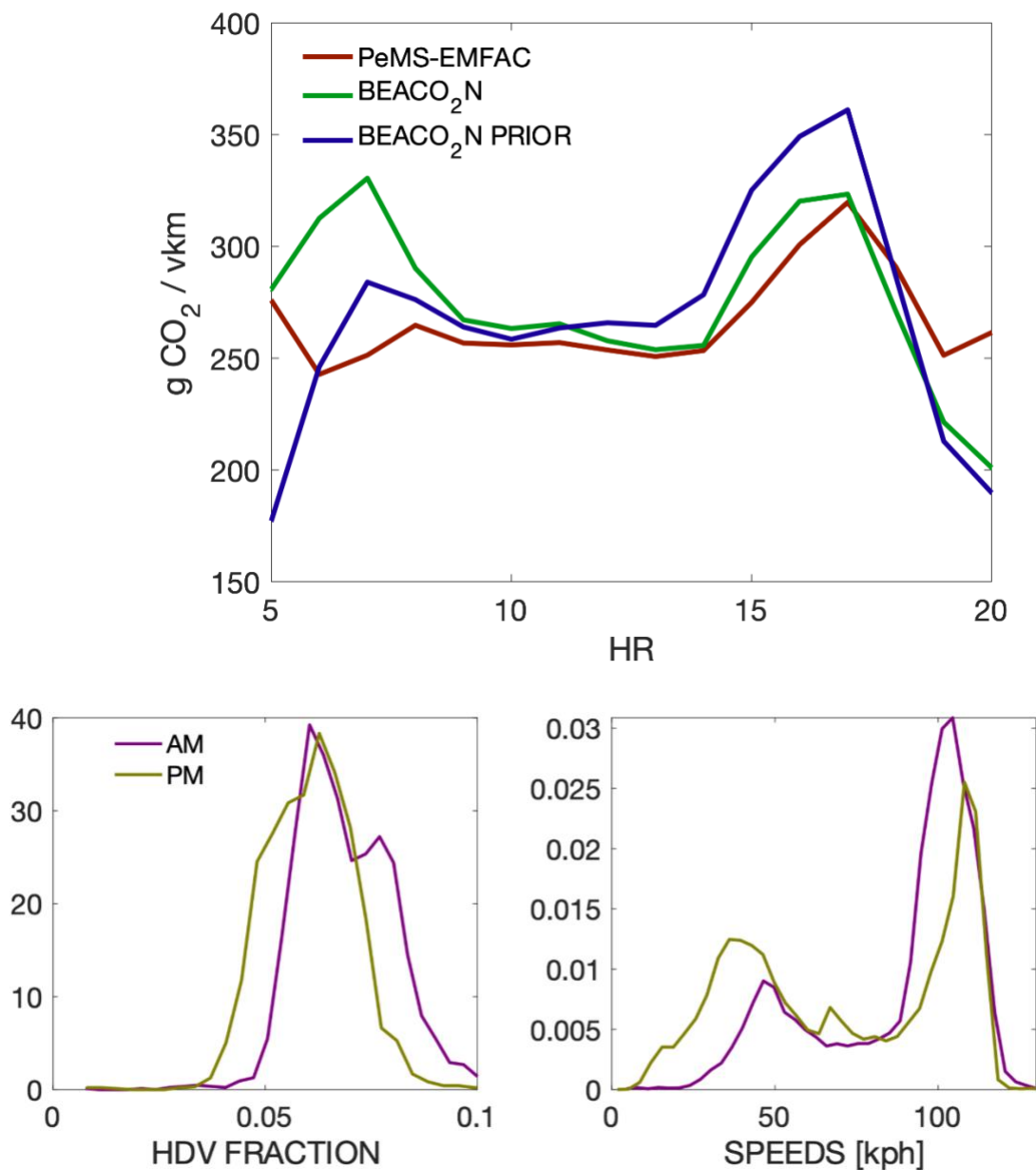


**Figure 4:** Top: Emissions rates by time of day on weekdays for PeMS-derived (red), BEACO<sub>2</sub>N-prior (blue), and  
375 BEACO<sub>2</sub>N posterior (green). Bottom: Probability density functions of truck fraction (left) and speed (right) from weekday  
morning (5-9 am) and evening (4-8 pm) rush hour period on the segment of I-80 analyzed in the Results section. Y-axis  
represents the relative probability of HDV fraction (left) or averaged hourly speed (right). Speeds are from individual PeMS  
sensors, while truck fraction is aggregated over the whole stretch under consideration (both directions).